

**AN ANALYSIS OF A FETI-DP ALGORITHM
ON IRREGULAR SUBDOMAINS IN THE PLANE
TR2007-889**

AXEL KLAWONN*, OLIVER RHEINBACH*, AND OLOF B. WIDLUND†

Abstract. In the theory for domain decomposition algorithms of the iterative substructuring family, each subdomain is typically assumed to be the union of a few coarse triangles or tetrahedra. This is an unrealistic assumption, in particular, if the subdomains result from the use of a mesh partitioner in which case they might not even have uniformly Lipschitz continuous boundaries. The purpose of this study is to derive bounds for the condition number of these preconditioned conjugate gradient methods which depend only on a parameter in an isoperimetric inequality and two geometric parameters characterizing John and uniform domains. A related purpose is to explore to what extent well known technical tools previously developed for quite regular subdomains can be extended to much more irregular subdomains. Some of these results are valid for any John domains, while an extension theorem, which is needed in this study, requires that the subdomains are uniform. The results, so far, are only complete for problems in two dimensions. Details are worked out for a FETI-DP algorithm and numerical results support the findings. Some of the numerical experiments illustrate that care must be taken when selecting the scaling of the preconditioners in the case of irregular subdomains.

Key words. domain decomposition, preconditioners, iterative substructuring, dual-primal FETI, John and uniform domains, fractal subdomains

AMS subject classifications. 65F10, 65N30, 65N55

1. Introduction. In the theory of domain decomposition methods of iterative substructuring type, we typically assume that each subdomain is quite regular, e.g., the union of a small set of coarse triangles or tetrahedra; see, e.g., [34, Assumption 4.3]. However, such an assumption is unlikely to hold especially if the subdomains result from using a mesh partitioner in which case the subdomain boundaries might not even be uniformly Lipschitz continuous, i.e., the number of patches which cover $\partial\Omega$, and in each of which the boundary is the graph of a Lipschitz continuous function, might not be uniformly bounded independently of the finite element mesh size. We also note that the shape of the subdomains are likely to change if the mesh size is altered and a mesh partitioner is used. The purpose of this paper is to develop a theory for domain decomposition methods under much weaker assumptions on the partitioning and to categorize the rate of convergence in terms of a few geometric parameters. We will denote the nonoverlapping subdomains by Ω_i and the interface between them by Γ .

So far, complete results have only been obtained for problems in the plane. To simplify our presentation, we will also focus on scalar elliptic problems of the following form:

$$-\operatorname{div}(\rho(x)\nabla u(x)) = f(x) \quad x \in \Omega, \quad (1.1)$$

with a homogeneous Dirichlet boundary condition on a measurable part, $\partial\Omega_D$, of $\partial\Omega$, the boundary of Ω , and a Neumann boundary condition on its complement $\partial\Omega_N$.

*Fachbereich Mathematik, Universität Duisburg-Essen, Universitätsstr. 3, 45177 Essen, Germany {axel.klawonn, oliver.rheinbach}@uni-due.de This work was supported in part by the Deutsche Forschungsgemeinschaft (DFG) under research grant KL 2094/1-1.

†Courant Institute, 251 Mercer Street, New York NY 10012, USA widlund@cims.nyu.edu This work was supported in part by the U.S. Department of Energy under contracts DE-FG02-06ER25718 and DE-FC02-01ER25482 and in part by National Science Foundation Grant DMS-0513251.

The coefficient $\rho(x)$ is strictly positive and assumed to be a constant ρ_i for $x \in \Omega_i$. As for many other algorithms, our results hold equally well for compressible elasticity problems in two dimensions; see [34, Chapter 8] for a discussion, [22] for further details on FETI–DP for linear elasticity, and the discussion below.

We use linear continuous finite elements and triangulations with shape regular triangles, i.e., the diameter of an element is bounded uniformly by a constant times the radius of the largest inscribed circle. We assume that each subdomain is a union of elements. We denote the finite element space on Ω by $W^h(\Omega)$ and assume that all elements vanish on $\partial\Omega_D$.

The analysis will be carried out for a FETI–DP algorithm but the results immediately carry over to the corresponding BDDC algorithm, see, e.g., [24], as well as to a class of inexact FETI–DP methods; see [20]. The tools that we will develop can also be used in the analysis of a number of other domain decomposition algorithms, in particular, those of [11, 12]; our study originated within this collaborative project with Clark Dohrmann. For a collection of auxiliary results used in the analysis of iterative substructuring algorithms, in the case of regular subdomains, see [34, Section 4.6].

Thus, our study requires the generalization of some technical tools used in the proof of bounds of the convergence rate of the FETI–DP algorithm. We also have to modify the basic line of reasoning in the proof of our main result; a proof for triangular subdomains and constant coefficients was first given in [27], see also [30, Chapter 2] for a proof more similar to ours. Four auxiliary results, namely a Poincaré inequality, a Sobolev-type inequality for finite element functions, bounds for certain edge terms, and a finite element extension theorem will be required in our proof; see Lemmas 2.3, 4.3, 4.4, and 4.5. We will work with *John domains* and *uniform domains*, see Definitions 2.1 and 2.4; the latter are also known as Jones or (ε, δ) -domains. We will express our bounds on the rate of convergence of our algorithm in terms of a few parameters identified in Definitions 2.1 and 2.4 and Lemma 2.2.

We will also consider the problem of linear, isotropic elasticity in two dimensions:

$$-\operatorname{div}(2\mu\varepsilon(\mathbf{u}) + \lambda\operatorname{tr}(\varepsilon(\mathbf{u}))I) = f \quad \text{in } \Omega \subset \mathbb{R}^2. \quad (1.2)$$

We assume zero Dirichlet conditions on one part of the boundary of $\partial\Omega$ with non-vanishing measure and traction conditions on the remaining part of the boundary. FETI–DP methods have been analyzed for linear elasticity and regular subdomains in [22]; see [19] and [21] for numerical results.

A crucial tool in any such study is the second Korn inequality, Lemma 2.6; for a proof for uniform domains, see Durán and Muschietti [14] and for John domain, see Acosta, Durán, and Muschietti [1]. The proof in [14] has many details in common to Jones’ proof of extension theorems for Sobolev spaces, [18], and the constant in the inequality depends only on the same geometric parameters as the result of Lemma 2.5.

The remainder of this article is organized as follows. In Section 2, we provide a Poincaré inequality for general domains and introduce John and uniform domains. In Section 3, we describe our FETI–DP algorithm and in Section 4, we develop a convergence theory for our FETI–DP algorithm for subdomains which are uniform. Finally, in Section 5, we present numerical results which confirm our theoretical findings. We note that we find a striking difference in the performance of the iterative method between the scaling based on our theory and another based on diagonal elements of the stiffness matrix in cases when the subdomain boundaries are highly irregular.

2. A Poincaré inequality, John and uniform domains. We will first introduce John domains and then consider a Poincaré inequality for such domains. Finally, we will introduce uniform domains; the latter are needed in order to prove an extension theorem. We note that this final assumption on the subdomains is not required in our analysis of domain decomposition algorithms based on overlapping subdomains; see [11, 12].

We next give the definition of a John domain; see [17] and the references therein. In the proofs of several of our auxiliary results, we will assume that the subdomains belong to this class.

DEFINITION 2.1 (John domain). *A domain $\Omega \subset \mathbb{R}^n$ – an open, bounded, and connected set – is a John domain if there exists a constant $C_J \geq 1$ and a distinguished central point $x_0 \in \Omega$ such that each $x \in \Omega$ can be joined to it by a rectifiable curve $\gamma : [0, 1] \rightarrow \Omega$ with $\gamma(0) = x_0$, $\gamma(1) = x$ and $|x - \gamma(t)| \leq C_J \cdot \text{distance}(\gamma(t), \partial\Omega)$ for all $t \in [0, 1]$.*

This condition can be viewed as a twisted cone condition. We note that certain snowflake curves with fractal boundaries are John domains, see Section 5, and that the boundary of a John domain can be arbitrarily much longer than its diameter.

The John condition allows us to estimate the diameter of the region Ω from above in terms of $|\Omega|^{1/n}$ and C_J ; it is elementary to prove that the diameter can be bounded from below and above in terms of $|\Omega|^{1/n}$ with one of the bounds depending on C_J . Restrictions on the boundary are of course also imposed.

In any analysis of any domain decomposition method with more than one level, we need a Poincaré inequality. This inequality is closely related to an isoperimetric inequality. The next lemma is due to Maz'ja [28] and Federer and Fleming [16]; see also Lin and Yang [25, Theorem 5.3.2] or Maz'ja [29].

LEMMA 2.2 (Isoperimetric inequality). *Let $\Omega \subset \mathbb{R}^n$ be a domain and let u be sufficiently smooth. Then,*

$$\inf_{c \in \mathbb{R}} \left(\int_{\Omega} |u - c|^{n/(n-1)} dx \right)^{(n-1)/n} \leq \gamma(\Omega, n) \int_{\Omega} |\nabla u| dx,$$

if and only if,

$$[\min(|A|, |B|)]^{1-1/n} \leq \gamma(\Omega, n) |\partial A \cap \partial B|. \quad (2.1)$$

Here, $A \subset \Omega$ is an arbitrary open set, and $B = \Omega \setminus \bar{A}$; $\gamma(\Omega, n)$ is the best possible constant and $|A|$ is the measure of the set A , etc.

We note that the domain does not need to be star-shaped or Lipschitz. It is known that if $\gamma(\Omega, 2)$ is bounded and the domain satisfies a certain separation property, then the domain must be a John domain; see [8]. For $n = 2$, the best choice of $c = \bar{u}_{\Omega}$, the average of u over the domain. A small value of $\gamma(\Omega, n)$ is desirable for our purposes.

In two dimensions, we immediately obtain the standard Poincaré inequality by using the Cauchy-Schwarz inequality.

LEMMA 2.3 (Poincaré's inequality). *Let Ω be a John domain in the plane. Then,*

$$\|u - \bar{u}_{\Omega}\|_{L_2(\Omega)}^2 \leq (\gamma(\Omega, 2))^2 |\Omega| \|\nabla u\|_{L_2(\Omega)}^2 \quad \forall u \in H^1(\Omega).$$

For $n = 3$ such a bound is obtained by using Hölder's inequality several times. In Lemma 2.3, we then should replace $|\Omega|$ by $|\Omega|^{2/3}$.

Throughout, we will use a weighted $H^1(\Omega_i)$ -norm defined by

$$\|u\|_{H^1(\Omega_i)}^2 = \int_{\Omega_i} \nabla u \cdot \nabla u dx + 1/H_i^2 \int_{\Omega_i} |u|^2 dx = |u|_{H^1(\Omega_i)}^2 + 1/H_i^2 \int_{\Omega_i} |u|^2 dx.$$

Here H_i is the diameter of Ω_i . The weight for the L_2 -term results from the standard H^1 -norm on a domain with diameter one and a dilation. We will use Lemma 2.3 to remove L_2 -terms in our estimates.

We finally define uniform domains. It is known, and easy to see, that any uniform domain is a John domain. It is also easy to construct John domains that are not uniform domains. According to Jones [18, Theorem 4], they form the largest class of domains for which an extension theorem holds in two dimensions; see Lemma 2.5 below. We note that it follows from [18, Theorem C] that if a domain is uniform, so is its complement.

DEFINITION 2.4 (Uniform domains). *A domain $\Omega \subset \mathbb{R}^n$ is a uniform domain if there exists a constant C_U such that any pair of points $x_1 \in \Omega$ and $x_2 \in \Omega$ can be joined by a rectifiable curve $\gamma(t) : [0, 1] \rightarrow \Omega$ with $\gamma(0) = x_1$, $\gamma(1) = x_2$, and where the Euclidean arc length of $\gamma \leq C_U|x_1 - x_2|$ and $\min_{i=1,2} |x_i - \gamma(t)| \leq C_U \cdot \text{distance}(\gamma(t), \partial\Omega)$ for all $t \in [0, 1]$. Note that domains with boundaries formed by von Koch curves as in Section 5 are also uniform domains.*

We will use a main result for uniform domains; see Jones [18, Theorem 1].

LEMMA 2.5. *Let $\Omega \subset \mathbb{R}^n$ be a uniform domain. There then exists a bounded, linear operator $E_\Omega : H^1(\Omega) \rightarrow H^1(\mathbb{R}^n)$, which extends any element in $H^1(\Omega)$ to one defined for all of \mathbb{R}^n , i.e., $(E_\Omega u)|_\Omega = u$ for all $u \in H^1(\Omega)$. The norm of this operator depends only on $C_U(\Omega)$ and the dimension n .*

As previously noted, for a result on linear elasticity, we also need a second Korn inequality for uniform domains; see Durán and Muschietti [14, Corollary 2.8].

LEMMA 2.6 (Korn inequality for uniform domains). *Let $\Omega \subset \mathbb{R}^n$ be a bounded uniform domain. Then, there exists a constant $C > 0$, which depends only on the uniformity constant $C_U(\Omega)$ and the dimension n , such that*

$$|\mathbf{u}|_{H^1(\Omega)}^2 \leq C \|\varepsilon(\mathbf{u})\|_{L_2(\Omega)}^2$$

for all $\mathbf{u} \in \{\mathbf{u} \in \mathbf{H}^1(\Omega) : \int_\Omega \left(\frac{\partial u_i}{\partial x_j} - \frac{\partial u_j}{\partial x_i} \right) dx = 0, i, j = 1, \dots, n\}$.

3. The FETI-DP algorithm. Let a domain $\Omega \subset \mathbb{R}^2$ be decomposed into N nonoverlapping subdomains Ω_i of diameter H_i , each of which is a union of finite elements with matching finite element nodes on the boundaries of neighboring subdomains across the interface $\Gamma := \bigcup_{i \neq j} \partial\Omega_i \cap \partial\Omega_j$. Here $\partial\Omega_i$ and $\partial\Omega_j$ are the boundaries of Ω_i and Ω_j , respectively. The interface Γ is the union of edges and vertices. The nodes on an edge are shared by exactly two subdomains and the edges are open subsets of Γ . The vertices are endpoints of the edges. For a more detailed definition of faces, edges, and vertices in two and three dimensions, see [22, Section 3] and [19, Section 2].

For each subdomain Ω_i , $i = 1, \dots, N$, we assemble the local stiffness matrices $K^{(i)}$ and load vectors $f^{(i)}$ from the contributions of the individual elements. We denote the vector of unknowns of the subdomain Ω_i by $u^{(i)}$ and we then partition the unknowns of $u^{(i)}$ into a vector of primal variables $u_{\Pi}^{(i)}$ and a vector of nonprimal variables $u_B^{(i)}$. We can obtain fast convergence by choosing only vertices as primal variables, since we are only considering two dimensional problems, see [15, 27, 30]. To simplify the description of the algorithm, we will assume that all vertices are primal. The nonprimal variables are those of $u_I^{(i)}$, associated with the interior nodes of the subdomain, and the dual displacement variables of the vector $u_{\Delta}^{(i)}$ associated with the remaining edge nodes. We will enforce the continuity of the solution in the primal

unknowns of $u_\Pi^{(i)}$ by making them global; we subassemble the subdomain stiffness matrices $K^{(i)}$ with respect to this set of variables and denote the resulting matrix by \tilde{K} . For all other interface variables, i.e., those of the $u_\Delta^{(i)}$, we will introduce Lagrange multipliers to enforce continuity.

Here are some more details: we partition the stiffness matrices according to the different sets of unknowns and obtain,

$$K^{(i)} = \begin{bmatrix} K_{BB}^{(i)} & K_{\Pi B}^{(i)T} \\ K_{\Pi B}^{(i)} & K_{\Pi\Pi}^{(i)} \end{bmatrix}, \quad K_{BB}^{(i)} = \begin{bmatrix} K_{II}^{(i)} & K_{\Delta I}^{(i)T} \\ K_{\Delta I}^{(i)} & K_{\Delta\Delta}^{(i)} \end{bmatrix},$$

and $f^{(i)T} = [f_B^{(i)T} \ f_\Pi^{(i)T}]$, $f_B^{(i)T} = [f_I^{(i)T} \ f_\Delta^{(i)T}]$.

We next define the block diagonal matrices

$$K_{BB} = \text{diag}_{i=1}^N(K_{BB}^{(i)}), \quad K_{\Pi B} = \text{diag}_{i=1}^N(K_{\Pi B}^{(i)}), \quad K_{\Pi\Pi} = \text{diag}_{i=1}^N(K_{\Pi\Pi}^{(i)}),$$

and load vectors $f_B^T = [f_B^{(1)T}, \dots, f_B^{(N)T}]$, $f_\Pi^T = [f_\Pi^{(1)T}, \dots, f_\Pi^{(N)T}]$.

Assembling the local subdomain matrices and load vectors with respect to the primal variables, we obtain the partially assembled global stiffness matrix \tilde{K} and the load vector \tilde{f} ,

$$\tilde{K} = \begin{bmatrix} K_{BB} & \tilde{K}_{\Pi B}^T \\ \tilde{K}_{\Pi B} & \tilde{K}_{\Pi\Pi} \end{bmatrix}, \quad \tilde{f} = \begin{bmatrix} f_B \\ \tilde{f}_\Pi \end{bmatrix},$$

where a tilde marks an assembled quantity. It is easy to see that, with all vertices primal, the matrix \tilde{K} is positive definite.

To enforce the continuity of the remaining interface variables $u_\Delta^{(i)}$, we introduce a jump operator B_B with entries 0, -1, or 1 and a vector of Lagrange multipliers λ . The FETI-DP saddlepoint problem is then given by

$$\begin{bmatrix} K_{BB} & \tilde{K}_{\Pi B}^T & B_B^T \\ \tilde{K}_{\Pi B} & \tilde{K}_{\Pi\Pi} & 0 \\ B_B & 0 & 0 \end{bmatrix} \begin{bmatrix} u_B \\ \tilde{u}_\Pi \\ \lambda \end{bmatrix} = \begin{bmatrix} f_B \\ \tilde{f}_\Pi \\ 0 \end{bmatrix}. \quad (3.1)$$

By eliminating u_B and \tilde{u}_Π from (3.1), we obtain

$$F\lambda = d, \quad (3.2)$$

with

$$F = B_B K_{BB}^{-1} B_B^T + B_B K_{BB}^{-1} \tilde{K}_{\Pi B}^T \tilde{S}_{\Pi\Pi}^{-1} \tilde{K}_{\Pi B} K_{BB}^{-1} B_B^T, \quad \tilde{S}_{\Pi\Pi} = \tilde{K}_{\Pi\Pi} - \tilde{K}_{\Pi B} K_{BB}^{-1} \tilde{K}_{\Pi B}^T,$$

and $d = B_B K_{BB}^{-1} f_B - B_B K_{BB}^{-1} \tilde{K}_{\Pi B}^T \tilde{S}_{\Pi\Pi}^{-1} (\tilde{f}_\Pi - \tilde{K}_{\Pi B} K_{BB}^{-1} f_B)$.

To define the Dirichlet preconditioner M , we need to introduce a scaled variant of the jump operator B_B , which we denote by $B_{B,D} = [B_{B,D}^{(1)}, \dots, B_{B,D}^{(N)}]$. The matrix $B_{B,D}^{(i)}$ is associated with the subdomain Ω_i and defined as follows: each row of $B_{B,D}^{(i)}$ with a nonzero entry corresponds to a Lagrange multiplier connecting the subdomain Ω_i with a neighboring subdomain Ω_j at a node $x \in \partial\Omega_{i,h} \cap \partial\Omega_{j,h}$. We obtain $B_{B,D}^{(i)}$ by multiplying each such row of $B_B^{(i)}$ by

$$\delta_i^\dagger := \frac{\rho_j}{\rho_j + \rho_i}; \quad (3.3)$$

see [22] or [34, Section 6.4] for further details. We will refer to this scaling as the ρ -scaling. The Dirichlet preconditioner is then given by

$$M^{-1} = B_{B,D}(R_{\Delta}^B)^T S_{\Delta\Delta} R_{\Delta}^B B_{B,D}^T, \quad \text{where}$$

$$S_{\Delta\Delta} = \text{diag}_{i=1}^N(S_{\Delta\Delta}^{(i)}), \quad S_{\Delta\Delta}^{(i)} = K_{\Delta\Delta}^{(i)} - K_{\Delta I}^{(i)}(K_{II}^{(i)})^{-1}K_{\Delta I}^{(i)T}, \quad \text{and } R_{\Delta}^B = \text{diag}_{i=1}^N(R_{\Delta}^{B(i)}).$$

The matrices $R_{\Delta}^{B(i)}$ are restriction operators with entries 0 or 1 which restrict the nonprimal degrees of freedom $u_B^{(i)}$ of a subdomain to its dual part $u_{\Delta}^{(i)}$.

Our FETI-DP method is the preconditioned conjugate gradient algorithm applied to the symmetric, positive definite system (3.2), using the preconditioner M^{-1} . We note that, as usual for iterative substructuring methods, the local Schur complements $S_{\Delta\Delta}^{(i)}$ do not have to be built explicitly. Instead local linear systems are solved in each iteration step.

4. Convergence theory. We recall that $W^h(\Omega_i)$ is the standard finite element space of continuous, piecewise linear functions on Ω_i which vanish on $\partial\Omega_D$. The corresponding finite element trace spaces are denoted by $W^{(i)} := W^h(\partial\Omega_i \cap \Gamma)$, $i = 1, \dots, N$. The product space of the $W^{(i)}$ is denoted by \widetilde{W} and its partially assembled subspace, with the primal variables global, is denoted by \widetilde{W} . We will denote by h_i the smallest diameter of the finite elements in the subdomain Ω_i .

We can now formulate our main result, which is also valid for compressible elasticity with Lamé parameters which are constant in each subdomain.

THEOREM 4.1 (Condition number estimate). *Let the domain $\Omega \subset \mathbb{R}^2$ be partitioned into subdomains which are uniform in the sense of Definition 2.4 and which are partitioned into shape regular elements. Then, with M the Dirichlet preconditioner, F the FETI-DP operator, and with h_i the smallest diameter of any element in Ω_i , the condition number of the conjugate gradient method satisfies*

$$\kappa(M^{-1}F) \leq C \max_i (1 + \log(H_i/h_i))^2.$$

Here C is a constant which depends only on the parameters $C_J(\Omega_i)$ and $C_U(\mathcal{C}\Omega_i)$ of Definitions 2.1 and 2.4, the Poincaré parameters $\gamma(\Omega_i, 2)$ of the subdomains, and the shape regularity of the finite elements.

We will denote by \mathcal{H} the discrete harmonic extension operator; $\mathcal{H}(v)$ is the minimal energy extension of the restriction of the finite element function v to the interface Γ . For each edge \mathcal{E}^{ij} , we also need to define an edge cut-off function $\theta_{\mathcal{E}^{ij}}$, which is the discrete harmonic function which equals 1 at all nodes on the edge \mathcal{E}^{ij} , common to Ω_i and Ω_j , and which vanishes at all other interface nodes.

In order to prove Theorem 4.1, we only need to establish the following result; see [22, Section 8] for a proof of a three-dimensional counterpart. We denote the restriction operator from \widetilde{W} to $W^{(i)}$ by $R^{(i)}$, $i = 1, \dots, N$.

LEMMA 4.2. *Let \mathcal{E}^{ij} be an edge common to the boundaries of Ω_i and Ω_j . For all $\tilde{w} \in \widetilde{W}$ and with $w^{(i)} := R^{(i)}\tilde{w}$, $w^{(j)} := R^{(j)}\tilde{w}$, we have*

$$\begin{aligned} \rho_i |\mathcal{H}(\theta_{\mathcal{E}^{ij}} \delta_i^\dagger (w^{(i)} - w^{(j)}))|_{H^1(\Omega_i)}^2 &\leq C(1 + \log(H_i/h_i))^2 \rho_i |w^{(i)}|_{H^1(\Omega_i)}^2 \\ &\quad + C(1 + \log(H_j/h_j))^2 \rho_j |w^{(j)}|_{H^1(\Omega_j)}^2. \end{aligned} \quad (4.1)$$

To prove this lemma, we need three auxiliary results, in addition to Poincaré's inequality. The first is a discrete Sobolev inequality. This inequality (4.2) is well-known

in the theory of iterative substructuring methods. Proofs for domains satisfying an interior cone condition are given in [6] and [7, Section 4.9] and a different proof is given in [34, page 102]. For a proof for John domains, see [12].

LEMMA 4.3 (Discrete Sobolev inequality). *Let $\Omega_i \subset \mathbb{R}^2$ be a John domain. Then,*

$$\|u - \bar{u}_{\Omega_i}\|_{L^\infty(\Omega_i)}^2 \leq C(1 + \log(H_i/h_i))^2 |u|_{H^1(\Omega_i)}^2, \quad (4.2)$$

for all $u \in W^h(\Omega_i)$. The constant C depends only on the John parameter $C_J(\Omega_i)$ of Ω_i and the shape regularity of the finite elements.

Another important tool provides estimates of certain edge terms. For regular subdomains in two dimensions, this lemma was first given in [13].

LEMMA 4.4 (Edge lemma). *Let Ω_i be a John domain, $\mathcal{E}^{ij} \subset \partial\Omega_i$ be an edge, and $\theta_{\mathcal{E}^{ij}} \in W^h(\Omega_i)$ be a finite element function which equals 1 at all nodes of \mathcal{E}^{ij} , vanishes at the other nodes on $\partial\Omega_i$, and is discrete harmonic in Ω_i . For $u \in W^h(\Omega_i)$, we have*

$$|\mathcal{H}(\theta_{\mathcal{E}^{ij}}u)|_{H^1(\Omega_i)}^2 \leq C(1 + \log(H_i/h_i))^2 \|u\|_{H^1(\Omega_i)}^2, \quad (4.3)$$

$$|\theta_{\mathcal{E}^{ij}}|_{H^1(\Omega_i)}^2 \leq C(1 + \log(H_i/h_i)), \quad (4.4)$$

and

$$\|\theta_{\mathcal{E}^{ij}}\|_{L_2(\Omega_i)}^2 \leq CH_i^2(1 + \log(H_i/h_i)). \quad (4.5)$$

Here, C depends only on the John parameter $C(\Omega_i)$ of Ω_i and the shape regularity of the finite elements. The logarithmic factor of (4.5) can be removed if all angles of the triangulation are acute.

Proof. We will establish inequality (4.3) by using ideas similar to those of [34, Proofs of Lemmas 4.24 and 4.25.]. We will construct a function $\vartheta_{\mathcal{E}^{ij}}$ which has the same boundary values as $\theta_{\mathcal{E}^{ij}}$ and which satisfies the two inequalities (4.3) and (4.4). Since $\theta_{\mathcal{E}^{ij}}$ and $\mathcal{H}(\theta_{\mathcal{E}^{ij}}u)$ are discrete harmonic, the two inequalities (4.3) and (4.4) will then hold. We note that $\vartheta_{\mathcal{E}^{ij}}$, which we will construct will not be a finite element function, and that the same is true for $\vartheta_{\mathcal{E}^{ij}}u$. But it is easy to see that the gradient of the finite element interpolant of $\vartheta_{\mathcal{E}^{ij}}$ will satisfy the same bound as $\nabla\vartheta_{\mathcal{E}^{ij}}$. We can also use [34, Lemma 4.31] to complete the argument for $\vartheta_{\mathcal{E}^{ij}}u$.

We first construct two curves, as in Definition 2.1, which connect the endpoints of the edge \mathcal{E}^{ij} to the point x_0 .

For each point of the curves, it is now possible to construct a circular disk, contained in Ω_i , with a radius as in Definition 2.1. We will replace this set by a union of rectangles contained in the union of a smaller family $\{B_k\}$ of disks creating two polygonal curves connecting the two end points of the edge. These two curves partition Ω_i into three parts. We will make $\vartheta_{\mathcal{E}^{ij}}$ identically 1 in the set next to the edge and make it vanish in the set most distant from the edge and we will bring the values of this function from 1 to 0 across the third, interior set.

The two John curves, that meet in x_0 , can be quite complicated. We will therefore replace them by the union of line segments which connect the centers of the family of circular disks B_k for each of the John curves. These disks, in turn, will be used to construct the family of rectangles $R_{k,k+1}$. We are able to estimate the sides of these rectangles as a function of the distance r to the closest endpoint of the edge \mathcal{E}^{ij} and we will use the union of these rectangles to construct a function $\vartheta_{\mathcal{E}^{ij}}$ with a bound on its gradient which is inversely proportional to r .

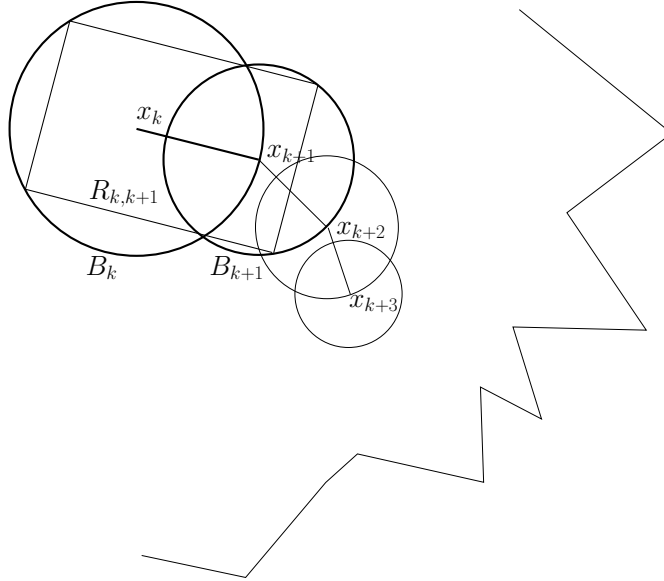


FIG. 4.1. The circular disks B_k and B_{k+1} , their centers x_k and x_{k+1} and the rectangle $R_{k,k+1}$.

The circular disks are constructed as in [12, Section 3] in which a number of properties are also derived; they are collected in Lemma 3.3 of the same paper. This material is essentially all borrowed from [17]. We will recall some of these results.

Let $\gamma(t)$ be one of the chosen John curves from the central point $x_0 \in \Omega_i$ to a vertex \mathcal{V} , one of the endpoint of the edge \mathcal{E}^{ij} . A family of circular disks B_k , $k \geq 0$ is introduced as follows: the first disk is $B_0 := B(x_0, \text{dist}(x_0, \partial\Omega)/4)$, the open set centered at x_0 and with radius $r_0 = \text{dist}(x_0, \partial\Omega)/4$. The other disks are defined similarly as $B_k := B(x_k, r_k)$, centered at x_k and with radius $r_k := |x - x_k|/(4C_J)$, $k \geq 1$. All the x_k lie on the John curve and all the B_k are subsets of Ω_i . Given B_k , we select $x_{k+1} \in \partial B_k$ as the last point of exit of $\gamma(t)$ from B_k .

The following properties are established in [12]: there exists a constant $M(C_J)$ such that

1. no point in Ω belongs to more than M disks;
2. the number of x_k that are at a distance larger than r from \mathcal{V} is bounded by $M \log(H/r)$;
3. $r_{k+1} \geq (4C_J - 1)/(4C_J + 1) r_k$.

Let the rectangle $R_{k,k+1}$ be the largest rectangle inscribed in the closure of $B_k \cup B_{k+1}$ and with two sides parallel to the line segment between x_k and x_{k+1} ; see Figure 4.1. Since x_{k+1} is on ∂B_k , one side of the rectangle is of length $2r_k$ and it is also easy to show, by using the lower bound on r_{k+1} , that the other is bounded from below by $C r_k$ where C is a positive constant independent of k . We also see that the distance from any point on $[x_k, x_{k+1}]$ to the boundary of the rectangle exceeds $C r_k$ for a constant $C > 0$ and the same bound clearly holds for the union of the rectangles.

We denote by $N(h)$ the index of the first x_k which lies in the union of the elements which have \mathcal{V} as a vertex. We take the union of all rectangles $R_{k,k+1}$ with $k < N(h)$ and the elements which have the subdomain vertex on its boundary. We then triangulate the resulting region using only nodes on the boundary of this set. We assign the value 1 to $\vartheta_{\mathcal{E}^{ij}}$ on the side of this set which is closest to the edge \mathcal{E}^{ij} and

let this function vanish on the other side. In between, we use linear interpolation on the triangulation, just constructed, to define $\vartheta_{\mathcal{E}^{ij}}$.

For each rectangle $R_{k,k+1}$, we can estimate the gradient of $\vartheta_{\mathcal{E}^{ij}}$ by C/r_k . Using Lemma 4.3, we then find that

$$|\vartheta_{\mathcal{E}^{ij}} u|_{H^1(R_{k,k+1})}^2 \leq C(1 + \log(H/h)) \|u\|_{H^1(\Omega_i)}^2.$$

The contributions from the elements which have the vertex \mathcal{V} as a vertex can be estimated quite easily. Inequality (4.4) now follows by using the estimate of the number of rectangles.

The estimate of $|\vartheta_{\mathcal{E}^{ij}}|_{H^1(\Omega_i)}$ follows from the same type of arguments.

For the $L_2(\Omega_i)$ -bound, we note that $\vartheta_{\mathcal{E}^{ij}} - \theta_{\mathcal{E}^{ij}}$ vanishes on the subdomain boundary and that we can estimate the $L_2(\Omega_i)$ -norm of $\vartheta_{\mathcal{E}^{ij}} - \theta_{\mathcal{E}^{ij}}$ in terms of the smallest eigenvalue of the Dirichlet problem for the Laplacian and the $H^1(\Omega_i)$ -bound just established. The bound for $\theta_{\mathcal{E}^{ij}}$ then follows from the trivial bound $\|\theta_{\mathcal{E}^{ij}}\|_{L_2(\Omega_i)} \leq |\Omega_i|^{1/2}$.

If all angles of the triangulation are acute, the finite element discretization will satisfy a maximum principle; see Ciarlet and Raviart [9]. Then $0 \leq \theta_{\mathcal{E}^{ij}} \leq 1$ and we can easily estimate the L_2 -norm of $\theta_{\mathcal{E}^{ij}}$ in same way as for $\vartheta_{\mathcal{E}^{ij}}$. \square

The next lemma was proven for Lipschitz domains and quite general conforming finite elements in Widlund [35], using a technique by Astrakhatsev [2]; see also Toselli and Widlund [34] for a different proof. Here, we present a proof for more general domains by different means. We note that, in essence, this is a result, for a quite irregular interface, on the classical Dirichlet-Neumann algorithm for two subdomains as introduced in [34, Section 1.3.3].

LEMMA 4.5 (Extension lemma). *Let Ω_i and Ω_j be subsets of \mathbb{R}^n and two subdomains with a common $(n-1)$ -dimensional interface \mathcal{E}^{ij} . Furthermore, let Ω_i be a uniform domain, let $V_i^h = \{v_h \in W^h(\Omega_i) : v_h(x) = 0 \text{ at all nodes of } \partial\Omega_i \setminus \mathcal{E}^{ij}\}$, and let $V_j^h = \{v_h \in W^h(\Omega_j) : v_h(x) = 0 \text{ at all nodes of } \partial\Omega_j \setminus \mathcal{E}^{ij}\}$. Then, there exists an extension operator*

$$E_{ji}^h : V_j^h \longrightarrow V_i^h,$$

with the following properties:

1. $(E_{ji}^h u_h)|_{\Omega_j} = u_h \quad \forall u_h \in V_j^h,$
2. $\|E_{ji}^h u_h\|_{H^1(\Omega_i)} \leq C \|u_h\|_{H^1(\Omega_j)} \quad \forall u_h \in V_j^h,$

where the constant $C > 0$ depends only on the uniformity parameter $C_U(\mathcal{C}\Omega_i)$ of the complement of Ω_i and the shape regularity of the finite elements and is otherwise independent of the finite element mesh sizes h_i and h_j and the diameters H_i and H_j .

Proof. The proof uses Lemma 2.5 and a result on finite element interpolation of nonsmooth functions given in Scott and Zhang [33]; see also Brenner and Scott [7, Section 4.8]. Their results represent a refinement of well known work by Clément [10].

From Lemma 2.5 and the fact that the complement of a uniform domain is uniform, we know that there exists an extension operator

$$E_{\mathcal{C}\Omega_i} : H^1(\mathcal{C}\Omega_i) \longrightarrow H^1(\mathbb{R}^n),$$

and a positive constant C , which depends only on the uniformity constant $C_U(\mathcal{C}\Omega_i)$, such that

$$\|E_{\mathcal{C}\Omega_i} u\|_{H^1(\mathbb{R}^n)} \leq C \|u\|_{H^1(\mathcal{C}\Omega_i)} \quad \forall u \in H^1(\mathcal{C}\Omega_i), \quad (4.6)$$

with $(E_{\mathcal{C}\Omega_i}u)|_{\mathcal{C}\Omega_i} = u$ for $u \in H^1(\mathcal{C}\Omega_i)$.

Let $\Omega_{ij} = \Omega_i \cup \Omega_j \cup \mathcal{E}^{ij}$. It is shown in Scott and Zhang [33] that there exists a boundary value preserving finite element interpolation operator

$$\Pi^h : H_0^1(\Omega_{ij}) \longrightarrow W^h(\Omega_{ij}) \cap H_0^1(\Omega_{ij}),$$

$$\text{with } \Pi^h v_h = v_h \quad \forall v_h \in W^h(\Omega_{ij}) \cap H_0^1(\Omega_{ij}), \quad (4.7)$$

$$\text{and } \|\Pi^h v\|_{H^1(\Omega_{ij})} \leq C \|v\|_{H^1(\Omega_{ij})} \quad \forall v \in H^1(\Omega_{ij}). \quad (4.8)$$

The constant C is independent of the mesh parameters and H_i and H_j . In their proof, Scott and Zhang construct a dual basis for the standard nodal basis of the finite element space in terms of integrals over elements or $(n-1)$ -simplices, i.e., edges in two and faces in three dimensions. There is a great deal of flexibility and, in particular, for each node - and its associated degree of freedom - one can choose any element of which it is a vertex. For all nodes in $\overline{\Omega}_j$, we select elements of Ω_j and for the nodes in $\overline{\Omega}_i \setminus \mathcal{E}^{ij}$ elements of Ω_i . This will guarantee that the values in $\overline{\Omega}_j$ will not be changed when the operator Π^h is applied; cf. (4.7).

Any finite element function $u_h \in V_j^h$ can now be extended by zero outside of Ω_{ij} . This extended function, \tilde{u} , has the same H^1 -norm as u_h . We next define

$$E_{j_i}^h u_h := \Pi^h(E_{\mathcal{C}\Omega_i} \tilde{u}),$$

and obtain, by using (4.6) and (4.8),

$$\|E_{j_i}^h u_h\|_{H^1(\Omega_i)} \leq C \|E_{\mathcal{C}\Omega_i} \tilde{u}\|_{H^1(\mathbb{R}^n)} \leq C \|\tilde{u}\|_{H^1(\mathcal{C}\Omega_i)} = C \|u_h\|_{H^1(\Omega_j)}.$$

The constant C depends only on the shape regularity of the finite elements and the uniformity constant $C_U(\mathcal{C}\Omega_i)$. By construction, we also have

$$(E_{j_i}^h u_h)|_{\Omega_j} = u_h \quad \forall u_h \in V_j^h.$$

□

We now present a proof of Lemma 4.2:

Proof. [Lemma 4.2] Consider an arbitrary $w \in \widetilde{W}$ and let $w^{(i)} := R^{(i)}w$ and $w^{(j)} := R^{(j)}w$. Our scaling factors (3.3) satisfy the following elementary estimate, see [22, Lemma 8.4],

$$\rho_i (\delta_i^\dagger)^2 = \rho_i \frac{\rho_j^2}{(\rho_i + \rho_j)^2} \leq \min\{\rho_i, \rho_j\}.$$

Proceeding as in [22] or [30], we find

$$\begin{aligned} & \rho_i |\mathcal{H}(\theta_{\mathcal{E}^{ij}} \delta_i^\dagger (w^{(i)} - w^{(j)}))|_{H^1(\Omega_i)}^2 \\ &= \rho_i |\mathcal{H}(\theta_{\mathcal{E}^{ij}} \delta_i^\dagger ((w^{(i)} - \bar{w}_{i,\Omega_i}) - (w^{(j)} - \bar{w}_{j,\Omega_j}) + (\bar{w}_{i,\Omega_i} - \bar{w}_{j,\Omega_j})))|_{H^1(\Omega_i)}^2 \\ &\leq 3 \min\{\rho_i, \rho_j\} \left(|\mathcal{H}(\theta_{\mathcal{E}^{ij}} (w^{(i)} - \bar{w}_{i,\Omega_i}))|_{H^1(\Omega_i)}^2 + |\mathcal{H}(\theta_{\mathcal{E}^{ij}} (w^{(j)} - \bar{w}_{j,\Omega_j}))|_{H^1(\Omega_i)}^2 \right. \\ &\quad \left. + |\theta_{\mathcal{E}^{ij}} (\bar{w}_{i,\Omega_i} - \bar{w}_{j,\Omega_j})|_{H^1(\Omega_i)}^2 \right). \end{aligned}$$

We have added and subtracted the averages $\bar{w}_{i,\Omega_i} = \int_{\Omega_i} w^{(i)} dx / \int_{\Omega_i} 1 dx$ and $\bar{w}_{j,\Omega_j} = \int_{\Omega_j} w^{(j)} dx / \int_{\Omega_j} 1 dx$. We can estimate the first term above using Lemmas 2.3 and 4.4 and find that,

$$\begin{aligned} & \min\{\rho_i, \rho_j\} |\mathcal{H}(\theta_{\mathcal{E}^{ij}}(w^{(i)} - \bar{w}_{i,\Omega_i}))|_{H^1(\Omega_i)}^2 \\ & \leq C(1 + \log(H_i/h_i))^2 \rho_i \|w^{(i)} - \bar{w}_{i,\Omega_i}\|_{H^1(\Omega_i)}^2 \\ & \leq C(1 + \log(H_i/h_i))^2 \rho_i |w^{(i)}|_{H^1(\Omega_i)}^2. \end{aligned}$$

We have the same type of bound for the second term. By using that the harmonic extension always has the least energy of all possible extensions, Lemma 4.5, and a Friedrichs inequality, we obtain

$$\begin{aligned} |\mathcal{H}(\theta_{\mathcal{E}^{ij}}(w^{(j)} - \bar{w}_{j,\Omega_j}))|_{H^1(\Omega_i)}^2 & \leq |E_{ji}^h(\mathcal{H}(\theta_{\mathcal{E}^{ij}}(w^{(j)} - \bar{w}_{j,\Omega_j})))|_{H^1(\Omega_i)}^2 \\ & \leq C \|\mathcal{H}(\theta_{\mathcal{E}^{ij}}(w^{(j)} - \bar{w}_{j,\Omega_j}))\|_{H^1(\Omega_j)}^2 \\ & \leq C |\mathcal{H}(\theta_{\mathcal{E}^{ij}}(w^{(j)} - \bar{w}_{j,\Omega_j}))|_{H^1(\Omega_j)}^2. \end{aligned}$$

We can then proceed exactly as for the first term.

There remains to estimate the third term:

$$|\theta_{\mathcal{E}^{ij}}(\bar{w}_{i,\Omega_i} - \bar{w}_{j,\Omega_j})|_{H^1(\Omega_i)}^2 = |\theta_{\mathcal{E}^{ij}}|_{H^1(\Omega_i)}^2 |\bar{w}_{i,\Omega_i} - \bar{w}_{j,\Omega_j}|^2.$$

The energy of $\theta_{\mathcal{E}^{ij}}$ is estimated in Lemma 4.4. Adding and subtracting the common value $w_{i,\mathcal{V}^{ik}} = w_{j,\mathcal{V}^{ik}}$ at a primal vertex \mathcal{V}^{ik} , which is an end point of \mathcal{E}^{ij} , we find that

$$|\bar{w}_{i,\Omega_i} - \bar{w}_{j,\Omega_j}|^2 \leq 2|\bar{w}_{i,\Omega_i} - w_{i,\mathcal{V}^{ik}}|^2 + 2|\bar{w}_{j,\Omega_j} - w_{j,\mathcal{V}^{ik}}|^2.$$

For the first term on the right hand side, we obtain using the discrete Sobolev inequality (4.2),

$$\begin{aligned} |w_{i,\mathcal{V}^{ik}} - \bar{w}_{i,\Omega_i}|^2 & \leq \|w^{(i)} - \bar{w}_{i,\Omega_i}\|_{L^\infty(\Omega_i)}^2 \\ & \leq C(1 + \log(H_i/h_i)) |w^{(i)}|_{H^1(\Omega_i)}^2. \end{aligned} \quad (4.9)$$

We can proceed in the same way with the second term. □

5. Numerical results. In this section, we present numerical results for some irregular (and regular) subdomains for the Poisson and linear elasticity problems in two dimensions using linear finite elements. In our FETI-DP algorithm, all subdomain vertices are primal and there are no additional primal variables. We solve the linear systems of equations by the conjugate gradient method until a relative residual reduction of $\text{rtol}=1e-10$ is reached. Our FETI-DP implementation [19] uses PETSc [4, 3, 5].

5.1. Geometries. We examine the effect of three different types of geometries. We first consider the case of the unit square, discretized using a structured mesh, and decomposed into 4×4 subdomains. We consider a regular, see Figure 5.2 (upper), and an irregular, ragged decomposition; see Figure 5.2 (lower) of this mesh. The irregular decomposition is constructed in the following way. We start with quadrilateral elements and the unit square decomposed into square subdomains. We then reassign some elements to neighboring subdomains in the following way: All elements, except

those touching the subdomain vertices, are reassigned in an alternating way. Each quadrilateral is then replaced by two triangles. Such ragged decompositions have previously been considered by Mandel, Dohrmann, and Tezaur [26].

We then consider 3×3 subdomains and an unstructured mesh. We consider a standard, regular decomposition, see Figure 5.4, and one where the interface Γ is defined in a recursive way; see Figure 5.3, as a fractal snowflake. These subdomains are obtained by first partitioning the unit square into smaller squares. We then replace the middle third of each edge by two other edges of an equilateral triangle, increasing the length of the interface by a factor $4/3$. The middle third of each of the resulting shorter edges is then replaced in the same way and this process is repeated until the desired refinement level is reached. This procedure gives us an interface which is snowflake-like; see Figure 5.1.

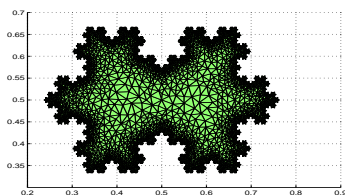


FIG. 5.1. A snowflake-shaped subdomain, recursion level 4.

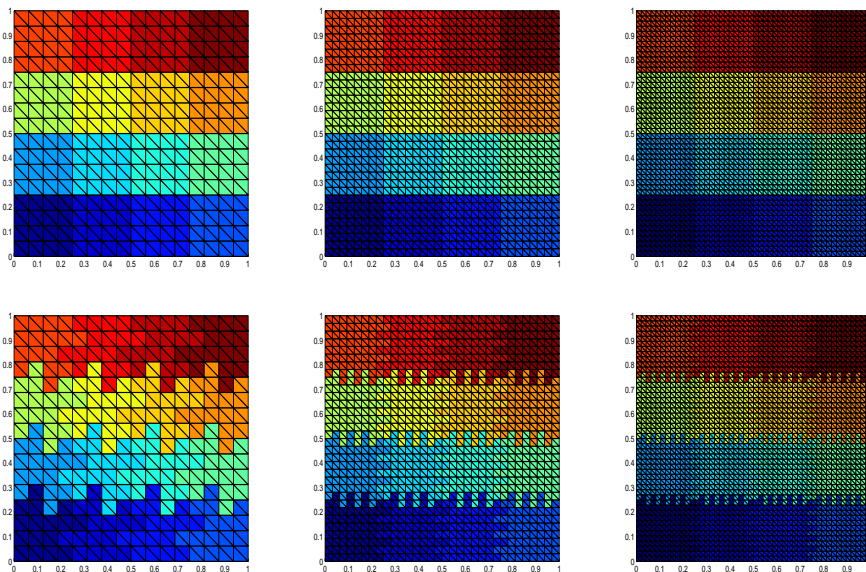


FIG. 5.2. Upper: Structured mesh, regular subdomains, $N=16$, $H/h=4,8,12$. Lower: Structured mesh irregular (ragged) subdomains, $N=16$, $H/h=4,8,12$.

5.2. Poisson's Equation. We first consider the Poisson problem for our different geometries using homogeneous Dirichlet boundary conditions and different values of H/h . For unstructured meshes, we approximate H/h by $(\text{dof})^{1/2}$, the square root

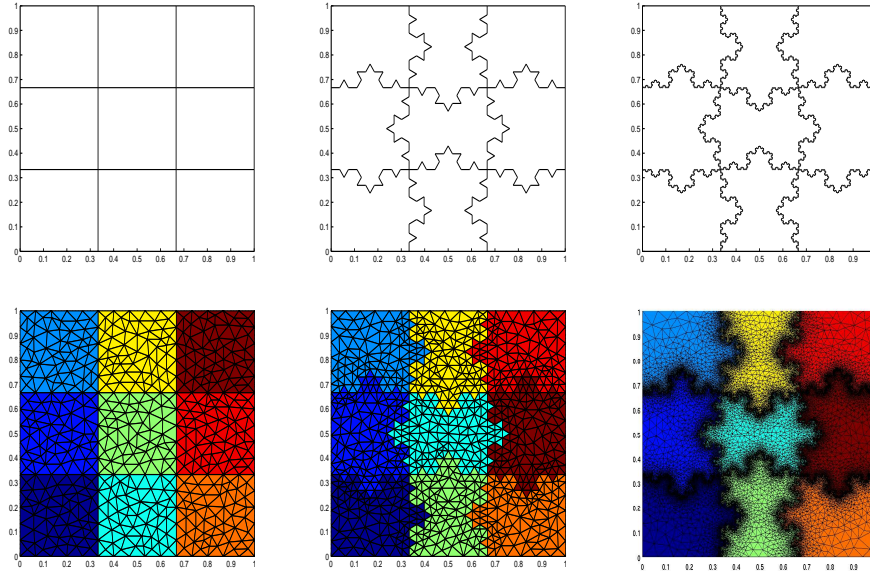


FIG. 5.3. *Unstructured mesh, irregular subdomains (snowflakes), $N=9$. Level 0, 2, and 4.*

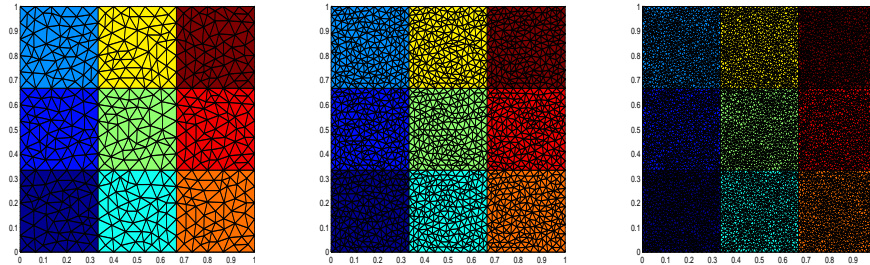


FIG. 5.4. *Unstructured mesh, regular subdomains, $N=9$. Refinement level 0, 1, and 2.*

of the total number of degrees of freedom. We compare the iteration numbers and the condition numbers for two different scalings. The ρ -scaling is the standard scaling as in (3.3) which uses the local coefficient of the PDE; see also [34, 23, 22]. The results of this paper are only valid for this type of scaling.

Since we treat only problems with constant coefficients, the ρ -scaling reduces to the multiplicity scaling of [31, 32]. We can therefore describe this scaling as follows: the multiplicity of a node is the number of subdomains it belongs to. The multiplicity scaling then scales the contribution from and to each node by the inverse of the multiplicity.

The stiffness scaling, cf. [31, 32], refers to a common practice in iterative substructuring codes which has been introduced for problems with variable coefficients to approximate the ρ -scaling. In the stiffness scaling, the diagonals of the local stiffness matrices are used to approximate the local coefficients. If we have constant coefficients, a structured mesh, and a regular decomposition into subdomains the stiffness scaling reduces to the multiplicity scaling but it does not for an irregular

decomposition.

Indeed, in the case of a structured mesh and a regular decomposition, see Figure 5.2 (upper), we get the same results for the two types of scalings, see Table 5.1, and the expected $C(1 + \log(H/h))^2$ behavior of the condition number; see Figure 5.6.

However, for an irregular decomposition, as in Figure 5.2 (lower), we find a significant deterioration of the condition number and the rate of convergence for increasing values of H/h , see Table 5.2 and Figure 5.5.

From Figure 5.5, we can see that for the ρ -scaling, we can again numerically confirm the expected $C(1 + \log(H/h))^2$ bound for the condition number. However, we see a linear growth in H/h of the condition number if stiffness scaling is used. The growth of the condition number is also reflected in the iteration count.

| Poisson: Structured Regular | | | | | | |
|-----------------------------|-----------|----------|--------|------|-------|------|
| H/h | total dof | Γ | ρ | | stiff | |
| | | | it | cond | it | cond |
| 4 | 289 | 84 | 4 | 1.63 | 4 | 1.63 |
| 8 | 1 089 | 180 | 5 | 2.22 | 5 | 2.22 |
| 16 | 4 225 | 372 | 6 | 2.96 | 5 | 2.96 |
| 32 | 16 641 | 756 | 7 | 3.84 | 7 | 3.84 |
| 64 | 66 049 | 1 524 | 7 | 4.85 | 7 | 4.85 |
| 128 | 263 169 | 3 060 | 8 | 6.02 | 8 | 6.02 |
| 192 | 591 361 | 4 596 | 9 | 6.76 | 9 | 6.76 |
| 256 | 1 050 625 | 6 132 | 8 | 7.31 | 8 | 7.31 |
| 320 | 1 640 961 | 7 668 | 11 | 7.75 | 11 | 7.75 |
| 368 | 2 362 369 | 9 204 | 11 | 8.13 | 11 | 8.13 |
| 448 | 3 214 849 | 10 740 | 11 | 8.45 | 11 | 8.45 |
| 512 | 4 198 401 | 12 276 | 10 | 8.73 | 10 | 8.73 |
| 576 | 5 313 025 | 13 812 | 11 | 8.99 | 11 | 8.99 |

TABLE 5.1

Poisson: Structured mesh, regular subdomains. ρ -scaling vs. stiffness scaling, $N=16$.

| Poisson: Structured Irregular (Ragged) | | | | | | |
|----------------------------------------|-----------|----------|--------|-------|-------|--------|
| H/h | total dof | Γ | ρ | | stiff | |
| | | | it | cond | it | cond |
| 4 | 289 | 180 | 19 | 4.95 | 15 | 3.21 |
| 8 | 1 089 | 468 | 23 | 6.50 | 18 | 5.27 |
| 16 | 4 225 | 1 044 | 24 | 7.45 | 21 | 9.75 |
| 32 | 16 641 | 2 196 | 25 | 8.47 | 25 | 20.36 |
| 64 | 66 049 | 4 500 | 26 | 9.61 | 32 | 44.74 |
| 128 | 263 169 | 9 108 | 27 | 10.89 | 41 | 100.07 |
| 192 | 591 361 | 13 716 | 27 | 11.70 | 48 | 159.88 |
| 256 | 1 050 625 | 18 324 | 27 | 12.32 | 54 | 222.50 |
| 320 | 1 640 961 | 22 932 | 28 | 12.82 | 60 | 287.20 |
| 368 | 2 362 369 | 27 540 | 28 | 13.24 | 65 | 353.54 |
| 448 | 3 214 849 | 32 148 | 28 | 13.60 | 70 | 421.25 |
| 512 | 4 198 401 | 36 756 | 28 | 13.92 | 74 | 490.13 |
| 576 | 5 313 025 | 41 364 | 28 | 14.20 | 77 | 560.02 |

TABLE 5.2

Poisson: Structured mesh, irregular subdomains. ρ -scaling vs. stiffness scaling, $N=16$.

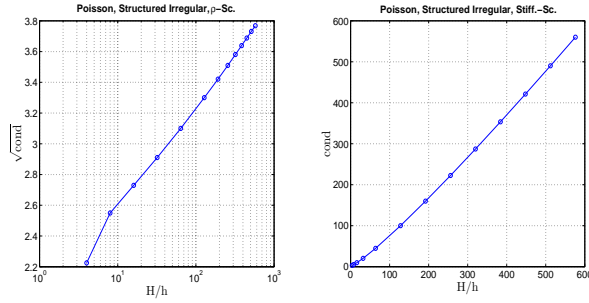


FIG. 5.5. Poisson (Table 5.2): Structured irregular (ragged), $N=16$. Left: ρ -scaling. Semilog Plot of $\sqrt{\text{cond}}$ vs. H/h ; Right: Stiffness scaling. Plot of cond vs. H/h .

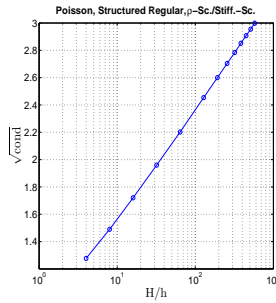


FIG. 5.6. Poisson (Table 5.1): Structured regular, $N=16$. Semilog plot of $\sqrt{\text{cond}}$ vs. H/h . ρ -scaling and stiffness scaling give identical results.

In order to verify that the condition number is independent of the number of subdomains for a fixed H/h also in the irregular case, we choose $H/h = 16$ in Table 5.3 and increase the number of subdomains N . We see that the iteration count as well as the condition numbers are indeed uniformly bounded.

| N | | | 16 | 64 | 256 | 1024 | 4096 |
|-----------|--------|------|------|-------|-------|-------|-------|
| Regular | ρ | cond | 2.96 | 3.28 | 3.35 | 3.38 | 3.38 |
| | | it | 6 | 14 | 16 | 16 | 15 |
| | stiff | cond | 2.96 | 3.28 | 3.35 | 3.38 | 3.38 |
| | | it | 6 | 14 | 16 | 16 | 15 |
| Irregular | ρ | cond | 7.45 | 8.01 | 8.13 | 8.12 | 8.10 |
| | | it | 24 | 27 | 30 | 29 | 29 |
| | stiff | cond | 9.75 | 10.62 | 10.60 | 10.75 | 10.73 |
| | | it | 21 | 27 | 31 | 31 | 30 |

TABLE 5.3
Poisson: Structured regular/irregular, condition number, $H/h=16$.

We then consider the case where we have an interface which is similar to a fractal snowflake. The finite element meshes are unstructured. We note that the number of nodes on the interface grows rapidly with the level of refinement of the snowflakes; cf. Tables 5.4 and 5.5. In spite of this, Tables 5.4 and 5.5, show that the condition number of the preconditioned FETI-DP operator only exceeds that of the trivial case by a factor of 3 resulting in a doubling of the number of conjugate gradient iterations if ρ -

scaling is used. Figure 5.7 indicates that the condition number satisfies a logarithmic bound in the square root of the total degrees of freedom. We also get such a bound for the unstructured regular case; see Table 5.5 and Figure 5.8.

In contrast, in the case where stiffness scaling is applied, the condition number is superlinear in the square root of the number of degrees of freedom.

| level | total dof | Γ | ρ | | stiff | |
|-------|-----------|----------|--------|-------|-------|----------|
| | | | it | cond | it | cond |
| 0 | 498 | 56 | 9 | 1.90 | 9 | 1.89 |
| 1 | 528 | 92 | 14 | 2.66 | 12 | 2.80 |
| 2 | 841 | 188 | 16 | 3.38 | 21 | 7.49 |
| 3 | 4 166 | 764 | 19 | 5.15 | 37 | 37.58 |
| 4 | 19 160 | 3 068 | 21 | 7.37 | 70 | 190.40 |
| 5 | 81 340 | 12 284 | 23 | 10.08 | 128 | 940.87 |
| 6 | 331 895 | 49 148 | 25 | 13.29 | 240 | 4 494.98 |

TABLE 5.4

Poisson: Unstructured mesh, irregular subdomains, $N=9$, ρ -scaling vs. stiffness scaling.

| total dof | Γ | ρ | | stiff | |
|-----------|----------|--------|------|-------|------|
| | | it | cond | it | cond |
| 398 | 56 | 8 | 1.90 | 9 | 1.89 |
| 1 688 | 104 | 8 | 2.40 | 10 | 2.39 |
| 5 430 | 200 | 10 | 3.04 | 12 | 3.07 |
| 21 513 | 404 | 11 | 3.83 | 13 | 3.95 |
| 85 641 | 812 | 12 | 4.75 | 15 | 4.94 |
| 341 745 | 1 628 | 13 | 5.79 | 16 | 6.06 |

TABLE 5.5

Poisson: Unstructured mesh, regular subdomains, $N=9$, ρ -scaling vs. stiffness scaling.

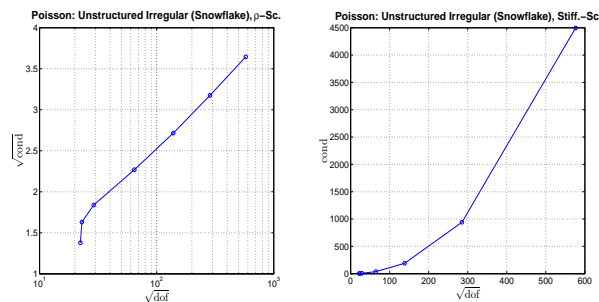


FIG. 5.7. Poisson (Table 5.4): Unstructured irregular (snowflake), $N=9$. Left: ρ -scaling. Semilog plot of $\sqrt{\text{cond}}$ vs. $\sqrt{\text{dof}}$. Right: Stiffness scaling. Plot of cond vs. $\sqrt{\text{dof}}$.

5.3. Elasticity. We have repeated all the experiments of Section 5.2 for the problem of linear elasticity. We essentially get the same results. We confirm the $C(1 + \log(H/h))^2$ bound for all cases where the ρ -scaling is applied, and we see a linear or even superlinear behavior in H/h of the condition number for the cases where the stiffness scaling is used with unstructured interfaces.

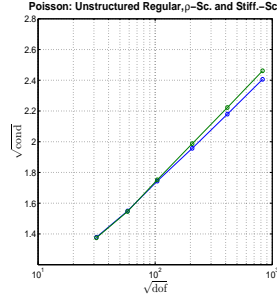


FIG. 5.8. Poisson (Table 5.5): Unstructured regular, $N=9$. Semilog plot of $\sqrt{\text{cond}}$ vs. $\sqrt{\text{dof}}$. ρ -scaling (lower curve) and stiffness scaling (upper curve) give similar results.

Elasticity: Structured Regular

| H/h | total dof | Γ | ρ | | stiff | |
|-----|------------|----------|--------|-------|-------|-------|
| | | | it | cond | it | cond |
| 4 | 578 | 168 | 12 | 2.11 | 12 | 2.11 |
| 8 | 2 178 | 360 | 14 | 2.97 | 14 | 2.97 |
| 16 | 8 450 | 744 | 17 | 4.03 | 17 | 4.03 |
| 32 | 33 282 | 1 512 | 20 | 5.30 | 20 | 5.30 |
| 64 | 132 098 | 2 048 | 22 | 6.78 | 22 | 6.78 |
| 128 | 526 338 | 6 120 | 24 | 8.73 | 24 | 8.72 |
| 192 | 1 182 722 | 9 192 | 26 | 10.32 | 26 | 10.32 |
| 256 | 2 101 250 | 12 264 | 27 | 11.35 | 27 | 11.35 |
| 320 | 3 281 922 | 15 336 | 29 | 12.19 | 29 | 12.19 |
| 368 | 4 724 738 | 18 408 | 30 | 12.90 | 30 | 12.90 |
| 448 | 6 429 698 | 21 480 | 31 | 13.52 | 31 | 13.52 |
| 512 | 8 396 802 | 24 552 | 30 | 14.07 | 30 | 14.07 |
| 576 | 10 626 050 | 27 624 | 32 | 14.56 | 32 | 14.56 |

TABLE 5.6

Elasticity: Structured mesh, regular subdomains, ρ -scaling vs. stiffness scaling, $N=16$.

Elasticity: Structured Irregular (Ragged)

| H/h | total dof | Γ | ρ | | stiff | |
|-----|------------|----------|--------|-------|-------|----------|
| | | | it | cond | it | cond |
| 4 | 578 | 360 | 39 | 19.42 | 27 | 10.98 |
| 8 | 2 178 | 936 | 60 | 33.93 | 42 | 19.45 |
| 16 | 8 450 | 2 088 | 66 | 38.87 | 51 | 33.11 |
| 32 | 33 282 | 4 392 | 69 | 41.69 | 61 | 65.72 |
| 64 | 132 098 | 9 000 | 70 | 45.06 | 77 | 139.13 |
| 128 | 526 338 | 18 216 | 71 | 48.87 | 103 | 299.05 |
| 192 | 1 182 722 | 27 432 | 72 | 51.29 | 121 | 468.50 |
| 256 | 2 101 250 | 36 648 | 72 | 53.07 | 138 | 644.49 |
| 320 | 3 281 922 | 45 864 | 73 | 54.52 | 156 | 825.07 |
| 368 | 4 724 738 | 55 080 | 73 | 55.71 | 169 | 1 009.14 |
| 448 | 6 429 698 | 64 296 | 74 | 56.77 | 180 | 1 196.07 |
| 512 | 8 396 802 | 73 512 | 74 | 57.67 | 195 | 1 385.60 |
| 576 | 10 626 050 | 82 728 | 74 | 58.50 | 204 | 1 577.28 |

TABLE 5.7

Elasticity: Structured mesh, irregular subdomains, ρ -scaling vs. stiffness scaling, $N=16$.

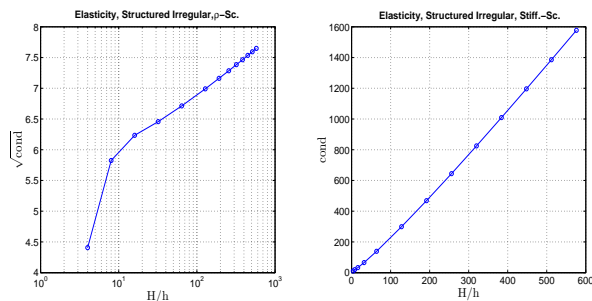


FIG. 5.9. Elasticity (Table 5.7): Structured irregular (ragged), $N=16$. Left: ρ -scaling. Semilog plot of $\sqrt{\text{cond}}$ vs. H/h . Right: Stiffness scaling. Plot of cond vs. H/h .

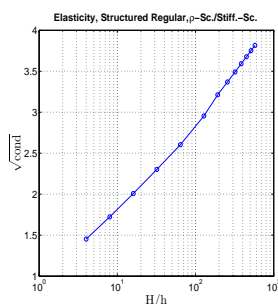


FIG. 5.10. Elasticity (Table 5.6): Structured regular, $N=16$. Semilog plot of $\sqrt{\text{cond}}$ vs. H/h . ρ -scaling and stiffness scaling give identical results.

| N | | | 16 | 64 | 256 | 1 024 | 4 096 |
|-----------|--------|------|-------|-------|-------|-------|-------|
| Regular | ρ | cond | 4.03 | 4.98 | 5.76 | 6.20 | 6.40 |
| | | it | 17 | 22 | 24 | 26 | 26 |
| | stiff | cond | 4.03 | 4.98 | 5.76 | 6.20 | 6.40 |
| | | it | 17 | 22 | 24 | 26 | 26 |
| Irregular | ρ | cond | 38.87 | 43.41 | 47.77 | 50.28 | 51.60 |
| | | it | 66 | 72 | 76 | 78 | 79 |
| | stiff | cond | 33.11 | 47.56 | 55.81 | 62.81 | 67.12 |
| | | it | 51 | 69 | 80 | 85 | 89 |

TABLE 5.8

Elasticity: Structured regular/irregular, condition number, $H/h=16$.

Acknowledgements. The authors are grateful to Professor Fanghua Lin of the Courant Institute for introducing the third author to John domains and Poincaré's inequality for very general domains. They also wish to thank Professors Piotr Hajłasz and Marcus Sarkis for interesting comments on our work.

REFERENCES

- [1] G. ACOSTA, R. G. DURÁN, AND M. A. MUSCHIETTI, *Solutions of the divergence operator on John domains*, Adv. Math., 206 (2006), pp. 373–401.
- [2] G. P. ASTRAKHATSEV, *Method of fictitious domains for a second-order elliptic equation with natural boundary conditions*, U.S.S.R. Computational Math. and Math. Phys., 18 (1978), pp. 114–121.

Elasticity: Unstructured Irregular (Snowflakes)

| level | total dof | Γ | ρ | | stiff | |
|-------|-----------|----------|--------|-------|-------|-----------|
| | | | it | cond | it | cond |
| 0 | 996 | 112 | 13 | 2.35 | 13 | 2.38 |
| 1 | 1 056 | 184 | 24 | 5.94 | 19 | 4.04 |
| 2 | 1 682 | 376 | 32 | 9.08 | 33 | 14.75 |
| 3 | 8 332 | 1 528 | 38 | 13.20 | 70 | 94.40 |
| 4 | 38 320 | 6 136 | 42 | 18.69 | 143 | 520.77 |
| 5 | 162 680 | 24 568 | 47 | 26.05 | 287 | 2 733.43 |
| 6 | 663 790 | 98 296 | 52 | 35.12 | 564 | 13 434.80 |

TABLE 5.9

Elasticity: Unstructured mesh, irregular subdomains, $N=9$, ρ -scaling vs. stiffness scaling.

Elasticity: Unstructured Regular

| total dof | Γ | ρ | | stiff | |
|-----------|----------|--------|------|-------|------|
| | | it | cond | it | cond |
| 992 | 112 | 13 | 2.35 | 13 | 2.38 |
| 3 376 | 208 | 15 | 3.05 | 15 | 3.10 |
| 10 860 | 400 | 17 | 3.95 | 17 | 4.12 |
| 43 026 | 808 | 19 | 5.17 | 20 | 5.49 |
| 171 282 | 1 624 | 21 | 6.72 | 22 | 7.16 |
| 683 490 | 3 256 | 24 | 8.54 | 25 | 9.12 |

TABLE 5.10

Elasticity: Unstructured mesh, regular subdomains, $N=9$, ρ -scaling vs. stiffness scaling.

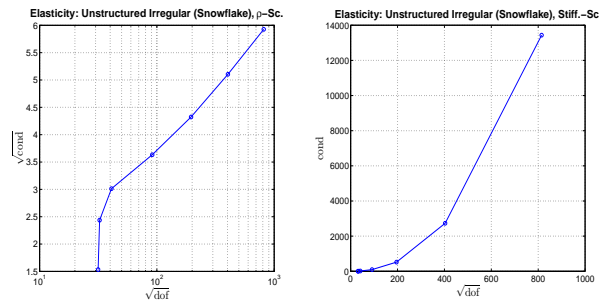


FIG. 5.11. *Elasticity (Table 5.9): Unstructured irregular (snowflakes), $N=9$. Left: ρ -scaling. Semilog plot of $\sqrt{\text{cond}}$ vs. $\sqrt{\text{dof}}$; Right: Stiffness scaling. Plot of cond vs. $\sqrt{\text{dof}}$.*

- [3] S. BALAY, K. BUSCHELMAN, V. EIJKHOUT, W. D. GROPP, D. KAUSHIK, M. G. KNEPLEY, L. C. MCINNES, B. F. SMITH, AND H. ZHANG, *PETSc users manual*, Tech. Rep. ANL-95/11 - Revision 2.1.5, Argonne National Laboratory, 2004.
- [4] S. BALAY, K. BUSCHELMAN, W. D. GROPP, D. KAUSHIK, M. G. KNEPLEY, L. C. MCINNES, B. F. SMITH, AND H. ZHANG, *PETSc Web page*, 2001. <http://www.mcs.anl.gov/petsc>.
- [5] S. BALAY, W. D. GROPP, L. C. MCINNES, AND B. F. SMITH, *Efficient management of parallelism in object oriented numerical software libraries*, in *Modern Software Tools in Scientific Computing*, E. Arge, A. M. Bruaset, and H. P. Langtangen, eds., Birkhäuser Press, 1997, pp. 163–202.
- [6] J. H. BRAMBLE, J. E. PASCIAK, AND A. H. SCHATZ, *The construction of preconditioners for elliptic problems by substructuring. I*, *Math. Comp.*, 47 (1986), pp. 103–134.
- [7] S. C. BRENNER AND L. R. SCOTT, *The Mathematical Theory of Finite Element Methods*, vol. 15 of *Texts in Applied Mathematics*, Springer-Verlag, New York, 2nd ed., 2002.
- [8] S. BUCKLEY AND P. KOSKELA, *Sobolev-Poincaré implies John*, *Math. Res. Lett.*, 2 (1995),

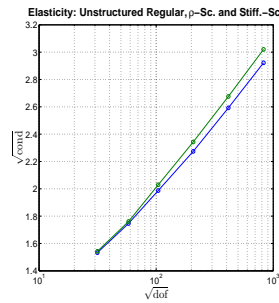


FIG. 5.12. Elasticity (Table 5.10): Unstructured regular, $N=9$. Semilog plot of $\sqrt{\text{cond}}$ vs. $\sqrt{\text{dof}}$, ρ -scaling (lower curve) and stiffness scaling (upper curve) give similar results.

- pp. 577–593.
- [9] P. G. CIARLET AND P.-A. RAVIART, *Maximum principle and uniform convergence for the finite element method*, Comput. Methods Appl. Mech. Engrg., 2 (1973), pp. 17–31.
- [10] P. CLÉMENT, *Approximation by finite element functions using local regularization*, Rev. Française Automat. Recherche Opérationnelle Sér. RAIRO Analyse Numérique, 9 (1975), pp. 77–84.
- [11] C. R. DOHRMANN, A. KLAWONN, AND O. B. WIDLUND, *A family of energy minimizing coarse spaces for overlapping Schwarz preconditioners*. Submitted to the proceedings of the 17th International Conference on Domain Decomposition Methods in Science and Engineering, Strobl, Austria, July 3-7, 2006, 2006.
- [12] ———, *Domain decomposition for less regular subdomains: Overlapping Schwarz in two dimensions*, Tech. Rep. TR2007-888, Department of Computer Science, Courant Institute of Mathematical Sciences, New York University, March 2007.
- [13] M. DRYJA AND O. B. WIDLUND, *Some domain decomposition algorithms for elliptic problems.*, in Iterative Methods for Large Linear Systems, L. Hayes and D. Kincaid, eds., Academic Press, 1989, pp. 273–291.
- [14] R. G. DURÁN AND M. A. MUSCHIETTI, *The Korn inequality for Jones domains*, Electron. J. Differential Equations, 2004 (2004), pp. 1–10.
- [15] C. FARHAT, M. LESOINNE, P. LE TALLEC, K. PIERSON, AND D. RIXEN, *FETI-DP: A dual-primal unified FETI method – part I: A faster alternative to the two-level FETI method*, Internat. J. Numer. Methods Engrg., 50 (2001), pp. 1523–1544.
- [16] H. FEDERER AND W. H. FLEMING, *Normal and integral currents*, Ann. of Math. (2), 72 (1960), pp. 458–520.
- [17] P. HAJLÁSZ, *Sobolev inequalities, truncation method, and John domains*, in Papers on analysis, vol. 83 of Rep. Univ. Jyväskylä Dep. Math. Stat., Univ. Jyväskylä, Jyväskylä, 2001, pp. 109–126.
- [18] P. W. JONES, *Quasiconformal mappings and extendability of functions in Sobolev space*, Acta Math., 147 (1981), pp. 71–88.
- [19] A. KLAWONN AND O. RHEINBACH, *A parallel implementation of Dual-Primal FETI methods for three dimensional linear elasticity using a transformation of basis*, SIAM J. Sci. Comput., 28 (2006), pp. 1886–1906.
- [20] ———, *Inexact FETI-DP methods*, Internat. J. Numer. Methods Engrg., 69 (2007), pp. 284–307.
- [21] ———, *Robust FETI-DP methods for heterogeneous three dimensional elasticity problems*, Comput. Methods Appl. Mech. Engrg., 196 (2007), pp. 1400–1414.
- [22] A. KLAWONN AND O. B. WIDLUND, *Dual-Primal FETI Methods for Linear Elasticity*, Comm. Pure Appl. Math., 59 (2006), pp. 1523–1572.
- [23] A. KLAWONN, O. B. WIDLUND, AND M. DRYJA, *Dual-Primal FETI methods for three-dimensional elliptic problems with heterogeneous coefficients*, SIAM J. Numer. Anal., 40 (2002), pp. 159–179.
- [24] J. LI AND O. B. WIDLUND, *FETI-DP, BDDC, and Block Cholesky Methods*, Internat. J. Numer. Methods Engrg., 66 (2006), pp. 250–271.
- [25] F. LIN AND X. YANG, *Geometric measure theory—an introduction*, vol. 1 of Advanced Mathematics (Beijing/Boston), Science Press, Beijing, 2002.
- [26] J. MANDEL, C. R. DOHRMANN, AND R. TEZAUER, *An algebraic theory for primal and dual*

- substructuring methods by constraints*, Appl. Numer. Math., 54 (2005), pp. 167–193.
- [27] J. MANDEL AND R. TEZAUER, *On the convergence of a dual-primal substructuring method*, Numer. Math., 88 (2001), pp. 543–558.
- [28] V. G. MAZ'JA, *Classes of domains and imbedding theorems for function spaces*, Soviet Math. Dokl., 1 (1960), pp. 882–885.
- [29] V. G. MAZ'JA, *Sobolev spaces*, Springer Series in Soviet Mathematics, Springer-Verlag, Berlin, 1985. Translated from the Russian by T. O. Shaposhnikova.
- [30] O. RHEINBACH, *Parallel scalable iterative substructuring: Robust exact and inexact FETI-DP methods with applications to elasticity*, PhD thesis, Department of Mathematics, University of Duisburg-Essen, July 2006.
- [31] D. RIXEN, *Substructuring and dual methods in structural analysis*, PhD thesis, University of Liège, Belgium, 1997.
- [32] D. RIXEN AND C. FARHAT, *A simple and efficient extension of a class of substructure based preconditioners to heterogeneous structural mechanics problems*, Internat. J. Numer. Methods Engrg., 44 (1999), pp. 489–516.
- [33] L. R. SCOTT AND S. ZHANG, *Finite element interpolation of nonsmooth functions satisfying boundary conditions*, Math. Comp., 54 (1990), pp. 483–493.
- [34] A. TOSELLI AND O. B. WIDLUND, *Domain Decomposition Methods - Algorithms and Theory*, vol. 34 of Springer Series in Computational Mathematics, Springer-Verlag, Berlin Heidelberg New York, 2005.
- [35] O. B. WIDLUND, *An extension theorem for finite element spaces with three applications*, in Numerical Techniques in Continuum Mechanics, W. Hackbusch and K. Witsch, eds., Braunschweig/Wiesbaden, 1987, Notes on Numerical Fluid Mechanics, v. 16, Friedr. Vieweg und Sohn, pp. 110–122. Proceedings of the Second GAMM-Seminar, Kiel, January, 1986.